

LATTICE QCD THREE-QUARK POTENTIAL ANALYSIS USING HYPERSPHERICAL VARIABLES REDUX: SAKUMICHI AND SUGANUMA DATA AND INTERPRETATION*

JAMES LEECH

University of St Andrews, The Old Burgh School
Abbey Walk, St Andrews, Fife KY16 9LB, Scotland, UK

MILOVAN ŠUVAKOV[†], V. DMITRAŠINOVIĆ

Institute of Physics, Belgrade University
Pregrevica 118, Zemun, P.O.Box 57, 11080 Beograd, Serbia

(Received June 23, 2020)

We analyze Sakumichi and Suganuma lattice QCD results for the 3-quark potential, using hyperspherical three-body coordinates. We show that their data supports neither the Delta, nor the Y-string interpretation, but something in-between. We show that the shape dependence of Sakumichi and Suganuma three-quark potential evaluated at $\beta = 5.8$ differs from the one evaluated at $\beta = 6.0$ by about 2%.

DOI:10.5506/APhysPolBSupp.14.215

1. Introduction

In spite of decades-long efforts [1–4], the functional form of the three-heavy-quark potential in lattice QCD is still not well known. Unlike the confining part of the two-body potential, which depends only on one variable — the distance between two bodies (quark and antiquark) — the three-body potential depends on three (scalar) variables.

Perhaps the simplest set of three-body variables that distinguishes permutation symmetric configurations are the hyperspherical coordinates, see [5, 6] and references therein, which consist of a (dimensional) hyperradius

* Presented at *Excited QCD 2020*, Krynica Zdrój, Poland, February 2–8, 2020.

[†] Currently on sabbatical leave of absence at: Department of Health Sciences Research, Mayo Clinic, 200 First Street SW, Rochester, MN 55905, USA.

$R = \sqrt{\frac{1}{3} \sum_{i < j}^3 (\mathbf{r}_i - \mathbf{r}_j)^2}$, which is proportional to the root-mean-square distance of the three particles from their geometrical barycenter $\mathbf{R}_{\text{gb}} = \frac{1}{3} \sum_i^3 \mathbf{r}_i$ (which equals the physical center-of-mass $\mathbf{R}_{\text{gb}} = \mathbf{R}_{\text{CM}}$ when all three masses are equal), and scales linearly with λ : $R \rightarrow \lambda R$, and thus measures the size of the system; and of two dimensionless (shape) variables, that may be expressed as hyperangles, or some functions thereof. The hyperangles $\phi = \arctan\left(\frac{2\rho \cdot \lambda}{\rho^2 - \lambda^2}\right)$ and $\alpha = \arccos\left(\frac{2(\rho \times \lambda)}{\rho^2 + \lambda^2}\right)$, defined in Ref. [6], are used here because they make the permutation symmetry manifest. The scaling transformation affects only the hyperradius, whereas the permutation symmetry affects only the two “shape space” variables/hyperangles.

2. Analysis of lattice data

In earlier publications [5, 6], we have analysed Koma and Koma and Takahashi *et al.* lattice results [2, 3] in terms of three hyperspherical coordinates. Whereas the old Takahashi *et al.* [3] data were insufficient to produce a continuous functional shape-space dependence, Koma and Koma [2] results yielded two smooth functions along two orthogonal lines in the shape space.

There are several important differences between Komas and Koma and Sakumichi calculations: [2] had a 24^4 lattice at $\beta = 6.0$ (lattice spacing $a = 0.093$ fm), with 221 three-quark geometries and only one gauge configuration; [1] had a $16^3 \times 32$ lattice at $\beta = 5.8$ (lattice spacing $a = 0.148(2)$ fm) with 101 three-quark geometries, and a $20^3 \times 32$ lattice at $\beta = 6.0$ (lattice spacing $a = 0.1022(5)$ fm) and 211 three-quark geometries, with 1000 and 2000 gauge configurations, respectively.

Figure 1 depicts all configurations of the three-body system in Ref. [1] including their permutations. The three lines that cross the origin represent isosceles triangles. Three lines orthogonal to them represent the right-angled triangles — one such line is at $y = -0.5$. One can see here that these lines are the only two sets of geometric configurations that are common to both the Koma and Suganuma data. We shall, therefore, use them both.

We assume that the total three-quark potential V_{3q} has the form of

$$V_{3q}(\alpha, \phi, R) = -\frac{A(\alpha, \phi)}{R} + B(\alpha, \phi)R + C, \quad (1)$$

henceforth referred to as the Coulomb + linear potential Ansatz. The first term represents the sum of QCD Coulomb pairwise interactions, which is dominant at small values of the hyperradius R . The second term represents the confinement potential, which is linear in R and dominant at large values of hyperradius R , and the third term — C — is a constant. Here, $A(\phi, \alpha)$ is assumed to be the (standard) sum of pair-wise Coulomb terms, and $B(\phi, \alpha)$

is the unknown hyperangular dependence of the linearly rising confining potential. Our goal is to determine $B(\phi, \alpha) \simeq V/R$ using the lattice data and the well-known hyperangular and hyperradial dependences of the two-body Coulomb term, as explained in Refs. [5, 6].

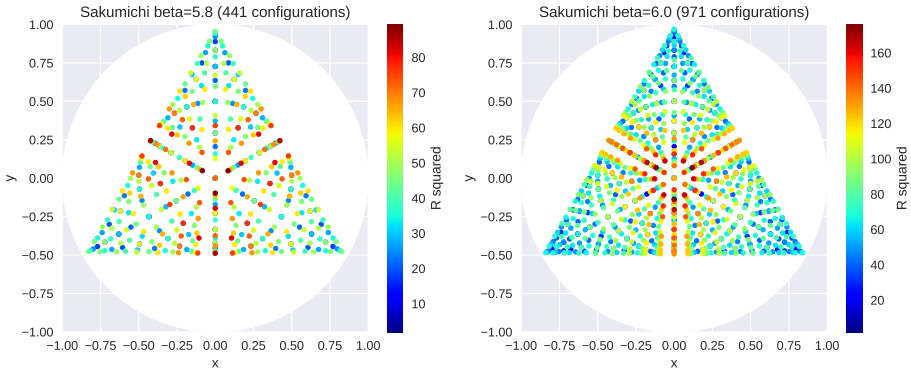


Fig. 1. Distribution of Sakumichi and Suganuma $3q$ configurations at $\beta = 5.8$ (l.h.s.) and $\beta = 6.0$ (r.h.s.).

We used the fixed equilateral triangle geometry with multiple sizes to fit the three free couplings A , B , C , see Table I.

TABLE I

Our and Sakumichi and Suganuma (taken from Table II in [1]) fitted constants in the 3-quark potential for equilateral triangles: the Coulomb coefficient $A = 3A_{3q}$, the string tension B , and the constant $C = C_{3q}$. Note the substantial difference of error bars.

β	A_{fit}	B_{fit}	C_{fit}	A_{Sak}	B_{Sak}	C_{Sak}
5.8	0.381(77)	0.166(6)	0.951(53)	0.357(9)	0.168(2)	0.93(1)
6.0	0.297(42)	0.088(2)	0.884(26)	0.363(9)	0.081(2)	0.936(9)

From Table I we can take the average values and the conservative error bars: $A = 0.369(77)$, $B = 0.167(6)$, $C = 0.94(5)$ at $\beta = 5.8$, and $A = 0.330(42)$, $B = 0.085(2)$, $C = 0.91(3)$ at $\beta = 6.0$. Note that the error bars of the Coulomb (A) and the constant term (C) are much larger (ranging from 21% for A , and 5% for C , to only 2.4% for B) than those for string tension B . We shall vary these constants, within their respective error bars, in our analysis so as to determine the dependence of the extracted shape dependences.

Case $\beta = 5.8$

It can be seen in Fig. 2(a) that for the isosceles triangle configurations in the [1] $\beta = 5.8$ data set, all of the $B(x)$ values form a scattered set of points, some of which, though not all, lie between the Δ and Y-string potentials' functional forms. As one imposes the hyperradial filter $R \geq 8.0$, the scatter reduces, as does the number of points, Fig. 2(b), but no single, smooth curve emerges. The corresponding graphs for the right-angled triangles are shown in Fig. 3. Note that most of the points fall between the (upper, black/blue) Δ -string prediction and the (lower, gray/red) Y-string, the only discrepancies being the multiple points near the isosceles right-angled configuration.

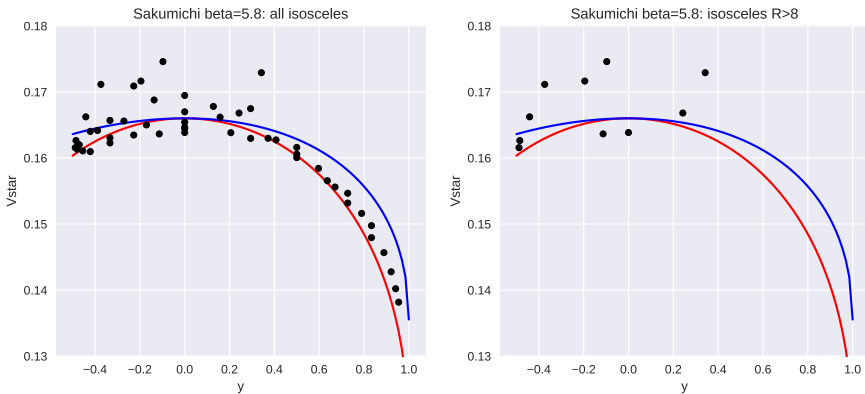


Fig. 2. (Color online) Extracted values of Sakumichi and Suganuma V/R for isosceles triangles ($y = 0$), at $\beta = 5.8$: (a) all (l.h.s); (b) with hyperradius filter $R \geq 8.0$ (r.h.s). The black/blue line represents the Δ -string, the gray/red line is the Y-string.

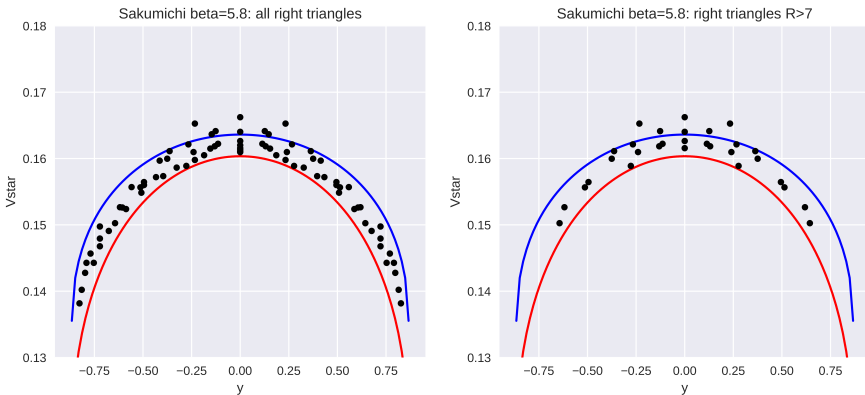


Fig. 3. (Color online) Extracted values of V/R for: (a) all right triangles ($x = 0.5$) (l.h.s); (b) right triangles ($x = 0.5$) with hyperradius filter $R \geq 7.0$, at $\beta = 5.8$, (r.h.s). The black/blue line represents the Δ -string, gray/red line is the Y-string.

Case $\beta = 6.0$

Similarly: (a) (again) the hyperradial filter $R \geq 8.0$ eliminates many widely scattered low- R points in Fig. 4, and many of the remaining points fall onto the (lower, gray/red) Y-string prediction in Fig. 5; (b) the resulting y dependence of $V(y)/R$ for right-angled triangles in Fig. 4 lies uniformly distributed between the Y-string and the Δ -string predictions, however.

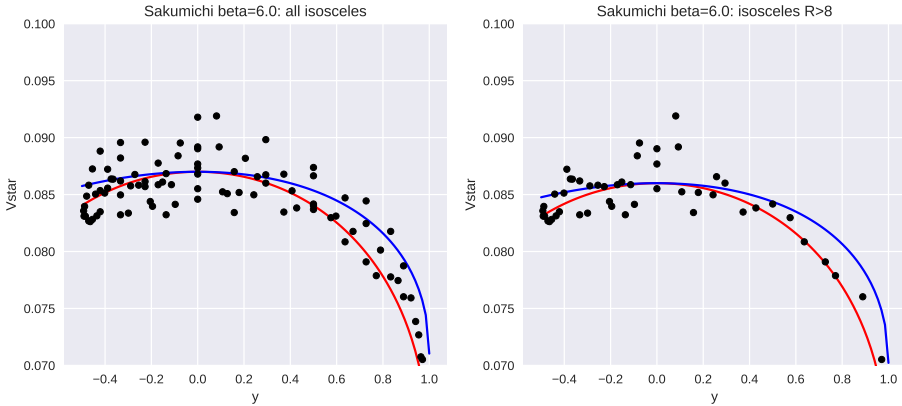


Fig. 4. Extracted values of V/R for: isosceles triangles ($y = 0$), at $\beta = 6.0$. (a) unrestricted data (l.h.s.); (b) with hyperradius filter $R \geq 9.0$. (r.h.s.).

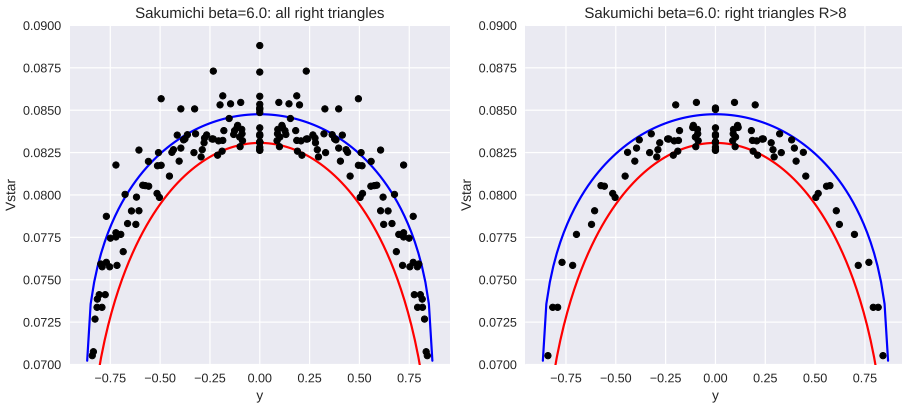


Fig. 5. Extracted values of V/R for: (a) all right triangles ($x = 0.5$) (l.h.s.); (b) right triangles ($y = 0$) with hyperradius larger than 8.0, at $\beta = 6.0$, (r.h.s.).

3. Conclusions

Comparing Fig. 4 with Fig. 2, we do not see major differences between the Sakumichi analyses for different β values. Figures 2 and 4 also show no major differences compared to the corresponding analyses [5, 6] of the Koma and Koma data set [2]. The shape-dependent part of the confining potential V/R must not change under scaling/renormalization, [7], therefore, the $\beta = 5.8$ and $\beta = 6.0$ functional dependences must be identical, which they are, within the uncertainties allowed by the error bars introduced in the fitting procedure.

We thank Naoyuki Sakumichi and Hideo Suganuma for providing unpublished details of their research. Some of this work was done while J.L. was visiting IPB on an IAESTE student exchange program. The work of M.Š. and V.D. was supported by the Serbian Ministry of Science and Technological Development under grant numbers OI 171037 and III 41011.

REFERENCES

- [1] N. Sakumichi, H. Suganuma, *Phys. Rev. D* **92**, 034511 (2015).
- [2] Y. Koma, M. Koma, *Phys. Rev. D* **95**, 094513 (2017).
- [3] T.T. Takahashi, H. Suganuma, Y. Nemoto, H. Matsufuru, *Phys. Rev. D* **65**, 114509 (2002).
- [4] C. Alexandrou, P. de Forcrand, A. Tsapalis, *Phys. Rev. D* **65**, 054503 (2002).
- [5] J. Leech, M. Šuvakov, V. Dmitrašinović, «Hyperspherical Three-Body Variables Applied to Lattice QCD Data», in: B. Dragovich, I. Salom, M. Vojinović (Eds.) «Proceedings of the Ninth Mathematical Physics Meeting», *Institute of Physics*, Belgrade, Serbia 2017, pp. 253–258.
- [6] J. Leech, M. Šuvakov, V. Dmitrašinović, *Acta Phys. Pol. B Proc. Suppl.* **11**, 435 (2018).
- [7] J. Smit, «Introduction to Quantum Fields on a Lattice: ‘a Robust Mate’», *Cambridge University Press*, Cambridge UK 2003.